

Article

pH and Heat Pretreatments with Zero-Valent Iron Addition to Enhance Biogas Production from Cassava Pulp Wastewater: Optimization and Comparison of Mathematical Models

Nittaya Boontian^{1,*}, Usa Yingchon¹ and Mohamad Padri^{1,2}

¹ School of Environmental Engineering, Suranaree University of Technology, Nakhon Ratchasima 30000, Thailand; usa_yingchon@hotmail.com (U.Y.)

² Development of Algal Biotechnology in Kingdom of Saudi Arabia (DAB-KSA) Project, Beacon Development, King Abdullah University of Science and Technology (KAUST), Thuwal 23955, Saudi Arabia

* Correspondence: n.boontian@sut.ac.th; Tel.: +66-4422-4584

Abstract: Pretreatments of pH and heat with zero-valent iron (ZVI) additions enhance anaerobic digestion and increase reducing sugar availability for optimum biogas production. This study aimed to optimize the conditions of different pH and heat pretreatment with additional ZVI to yield higher biogas amounts from the anaerobic digestion (AD) of cassava wastewater. Thirteen pH conditions, ten ZVI concentrations, and eleven heating periods were varied and measured to optimize the standard conditions. Four mathematical models that are widely used to evaluate the cumulative biogas production were employed, namely, the Modified Gompertz, Logistic, Transference, and Exponential models. The pretreatment of pH 10 and 35 min of boiling time with a ZVI concentration of 60 g·kg·TVS⁻¹ produced the highest cumulative biogas at the end of the AD process. The Logistic and Modified Gompertz models were better fitted with the experimental data than the other models. Interestingly, the optimized conditions altered the biogas production rate but prolonged the lag phase. A reasonably positive correlation was also found between the FeOOH amount and biogas production rate in the LF and MG models. These optimal fitted models, kinetics parameters, and possible correlations are novel findings that can help develop extensive scale developments for biogas generation from cassava wastewater.

Keywords: anaerobic digestion; pretreatments; zero-valent iron; mathematical models; biogas production



Citation: Boontian, N.; Yingchon, U.; Padri, M. pH and Heat Pretreatments with Zero-Valent Iron Addition to Enhance Biogas Production from Cassava Pulp Wastewater: Optimization and Comparison of Mathematical Models. *Fermentation*

2023, 9, 622. <https://doi.org/10.3390/fermentation9070622>

Academic Editor: Mohammad Taherzadeh

Received: 29 May 2023

Revised: 27 June 2023

Accepted: 28 June 2023

Published: 30 June 2023



Copyright: © 2023 by the authors. Licensee MDPI, Basel, Switzerland. This article is an open access article distributed under the terms and conditions of the Creative Commons Attribution (CC BY) license (<https://creativecommons.org/licenses/by/4.0/>).

1. Introduction

Cassava industry effluent has been widely utilized for biogas generation to remove excess nutrients that may harm the environment and, at the same time, provide renewable energy through an anaerobic digestion process (AD) [1–3]. It can supply a considerable amount of energy and reduce the total cost of the cassava industry by compensating for the high energy demand in the starch extraction process [2]. Several advancements in pretreatment and digestion processes have been developed to enhance the digestion process to maximize substrate utilization and wastewater treatments [4]. The pretreatments ensure the digestibility of the substrate, create a suitable environment for the microbial community, and increase the methane production rate [5]. The pretreatments also raise the possibility of higher methane percentage in biogas under efficient organic matter conversion via hydrolysis and the following processes [6].

Numerous pretreatment methods are available for cassava industry waste and wastewater when considering its high proportion of structural carbohydrates and lignin [7]. Mechanical, chemical, biological, physical, and thermal pretreatments were reported to have various effects on the biogas generation and organic matter removals in anaerobic digestion [4,8]. Among the pretreatments, thermal and chemical pretreatments have been proven

to be the most optimum and cost-effective methods for preparing the wastewater before conducting the anaerobic digestion [9,10]. Many studies reported the results of pH conditions during the heat pretreatments on anaerobic digestion in the various temperatures on biogas production. The acid condition using H_2SO_4 at 157.86°C for 20.15 min pretreatments showed $248\text{ mL}\cdot\text{g}^{-1}\cdot\text{VS}^{-1}$ of methane production from cassava residues [11]. However, it is essential to note that the extreme temperature in the pretreatment may result in inhibition of the byproducts that later can potentially reduce the biogas production at the later stage of methanogenesis [12]. Similarly, a maximum methane yield of $324 \pm 5\text{ mL}\cdot\text{gVS}^{-1}$ was achieved by adding 2.0% NaOH as pretreatment [13].

Furthermore, metals, such as Cu, Fe, Ni, Cd, and Zn, are often added to the system as an additive to increase biogas production in the AD [14]. Metals were reported to increase biogas production in low concentrations but highly inhibited the process in excess amounts [14,15]. Among the metals, iron ions, especially zero-valent iron (ZVI), are often added to the AD to enhance methanogen activity. Iron reacts with pyruvate metabolism enzymes and the cofactors of dehydrogenase enzymes to enhance biogas production [16,17]. ZVI was also reported to stimulate microbial metabolic performance and decrease the oxidation–reduction potential (ORP) [18]. Additionally, it is also applied as a reductive material in the wastewater treatment system and reacts well with hydrogen sulfide (H_2S) to form iron sulfide (FeS) to improve biogas quality [19,20]. ZVI was also reported to increase the hydrolysis bacteria community and alleviate acidification, thus resulting in a CH_4 yield increase of 77.3% [21]. It has also been reported that Fe^0 acts as an electron donor to decrease CO_2 and create suitable acetate formation for the microbial community in the system [22]. This result is due to the activity of ZVI that provides extra electrons, ferrous ions, and ferric ions to promote hydrolysis, acidogenesis, and acetogenesis bacteria [23]. Although these iron ions are essential in determining the increase of biogas generation, the forms and compositions of the iron ions after the AD are rarely studied, mainly in combination with the pretreatments [24].

The application of ZVI and heat combined in the pH pretreatment has been previously performed in other substrates. A study using alkaline pretreatment with heat and additional ZVI into waste activated sludge has resulted an increase of 95% of methane production [25]. Another form of iron (magnetite) has also been applied to rice straw after alkaline pretreatment to obtain an increase of 120% after the combination of the pretreatment and additional iron. In contrast, it has been also found that ZVI can act as a buffer to maintain process through which the pH can be stable throughout the anaerobic process and provide suitable conditions for the methanogens in palm oil mill effluent [23]. On the other hand, acid pretreatment has never been combined with ZVI addition. However, promising results have been achieved from previous studies using acid pretreatments to breakdown the complex of polysaccharides in the various substrates and to ease hydrolysis production [26–28]. However, the suitable pH condition during the pretreatment can vary based on the characteristics of the substrate and the process of the anaerobic digestion [29]. Thus, it is important to have sufficient experiments based on the actual substrate.

Cassava has become an important commodity in many tropical countries when considering its fast growth and the versatile utilization of the tuber. Cassava pulp wastewater is produced as residual product of cassava starch production. As it comes from the plant-based raw material, the structures mostly consist of lignocellulose and cellulose in which the degradation process may be limited before the process of anaerobic digestion [30]. The wastewater from the cassava starch industry is often treated inefficiently. The main treatment for this wastewater is anaerobic digestion. However, the effluent for this treatment often still possesses high contents of organic matter [31]. This is caused by the improper hydrolysis process in the initial stage of hydrolysis, which results in the failure of methanogens to utilize maximum carbon sources in the cassava residual [13]. Lignocellulose, a main constituent in the cassava wastewater, must be pretreated before undergoing any anaerobic pretreatment. It is important to ensure that cellulose and hemicellulose are released from the lignin to increase the waste degradability [11]. Moreover, the pretreated

cassava wastewater can still be enhanced to produce higher methane yields with regard to its high carbon source contents by enhancing the methanogenesis process [32]. Thus, it is important to develop a combination of pretreatments using the optimum condition with additional enhancement during the process of hydrolysis. As previously mentioned, the optimization of the pH condition during heat pretreatment in several durations may address the problem of the availability of the carbon source. On the other hand, additional ZVI may lead to a higher efficiency in converting the degradable substrate into methane.

The production of biogas and the removal of organic matter, often called the chemical oxygen demand (COD) value, are among the main focuses examining the pretreatment efficiency and the addition of metals [26,33]. From the previous studies, high COD removal efficiencies were often calculated from lengthy and inefficient pretreatment application processes when applied in the actual scale operation. Here, kinetics parameters are introduced to design the system and thus affect the operation performance. Several kinetics parameters from mathematical models must be understood entirely in the batch system before the continuous system is adopted [34]. Mathematical models have been developed to measure the kinetics of the operation conditions, including the effects of pretreatments and additives on AD. First-Order Kinetic [26,35], Modified Gompertz [15,35], Reaction-Curve-Type [35], Logistic Function [36,37], Exponential Rise to Maximum [35,38], and Gaussian models [39] are among the models that are often used for cumulative biogas production. The models can help when it comes to better understanding the process and holistic advantages of the pretreatments and the addition of metals into the system [36]. Nevertheless, no extensive study has previously examined these models' relations with the enhancement after pretreatments with ZVI addition.

To address the gaps mentioned above, this study aimed to perform and analyze biogas production from cassava pulp wastewater after the combination of pH adjustment and the duration of heat application for pretreatment with the addition of ZVI. The application of mathematical models to generate different kinetics parameters was also conducted. Moreover, the results were also tested to observe any possible correlations between effluent characteristics and the kinetics parameters. This approach has never been studied before but is advantageous as a potential tool to understand the mechanism of the pretreatment pretreatments with ZVI addition to generate methane production.

2. Materials and Methods

2.1. Wastewater Sources and Characterizations

Cassava pulp wastewater was collected from Korat Flour Industry Co., Ltd., Nakhon Ratchasima, Thailand (N 14°53053'' E 102°04000'') as the waste from the starch extraction process in cassava tuber, while the seed was obtained from the Lagoon Tank Sediment from the same industry. The seed was the inoculum of the microorganism community that could conduct and/or initiate the anaerobic digestion process. Wastewater characteristics, namely, biological oxygen demand (BOD), chemical oxygen demand (COD), volatile fatty acids (VFAs), alkalinity (Alk), total phosphorus (TP), orthophosphate (Orto-P), total kjeldahl nitrogen (TKN), total solids (TSs), volatile suspended solids (VSSs), and total volatile solids (TVSSs), were analyzed based on standard methods [40], while other physicochemical characteristics of the wastewater, such as pH level, were measured using a YSI 556 MPS Multiprobe System (Xylem, OH, USA). The results of seed and wastewater characterization are summarized in Table 1. The ratio between substrate and seeds was 0.08 [41].

Table 1. Cassava pulp wastewater and seed characteristics.

Wastewater	
Parameters	Mean ± sd
pH	4.23 ± 0.24
BOD (mg·L ⁻¹)	42,000 ± 6879
COD (mg·L ⁻¹)	55,400 ± 6116
VFA (mg·CH ₃ COOH·L ⁻¹)	161.67 ± 25
Alkalinity (mg·CaCO ₃ ·L ⁻¹)	336.67 ± 26
TP (mg·L ⁻¹)	70.86 ± 12
Orto-P (mg·L ⁻¹)	54.90 ± 2.89
TKN (mg·L ⁻¹)	393.52 ± 63.08
TS (%)	23.73 ± 3.90
TVS (%)	79.56 ± 10.41
Seed	
Parameters	Mean ± sd
pH	4.13 ± 0.65
BOD (mg·L ⁻¹)	42,000 ± 3927
TS (mg·L ⁻¹)	40,465 ± 1889
TVS (mg·L ⁻¹)	38,336 ± 6574
VSS (mg·L ⁻¹)	37,936 ± 2814
VFA (mg·CH ₃ COOH·L ⁻¹)	140 ± 7.59
Alkalinity	716 ± 47.90

2.2. Reactor Design

A two-tank reactor was occupied throughout the study to obtain the biogas from the AD process. The reactor was a 6 L batch reactor consisting of an AD tank, gas tank, and measurement glass (Figure 1a). Briefly, the AD tank was used for biogas generation, where substrate, seeds, and additives were added and mixed. It is the closed tank where the ambient air cannot enter to avoid any toxic gas disrupting the AD process. The AD was conducted in this tank, and the gasses from the AD were distributed to the gas tank via a silicon channel. The gas from the AD tank generates the pressure that displaces the water equal to the generated gas volume and the water was flowed into the measurement glass. The measurement of liquid was interpreted as the total biogas generated from the system. The AD tank was also equipped with a pH probe, gas collector channel, and an effluent valve to sample the substrates. Furthermore, the collected gas was analyzed using the channel and eventually analyzed using gas chromatography. The pH probe also collected the frequent data of the pH condition in the system.

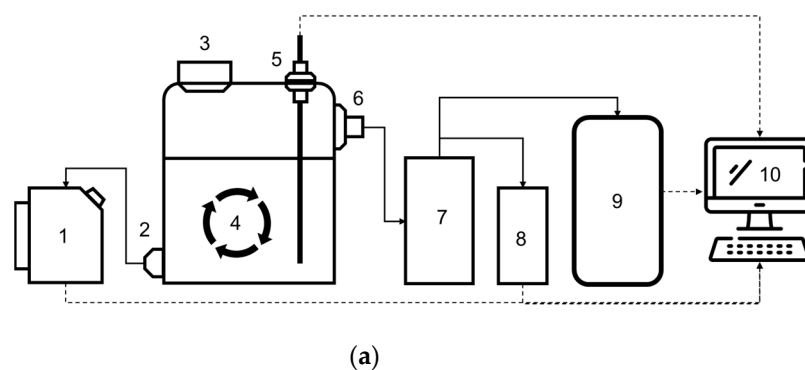


Figure 1. Cont.

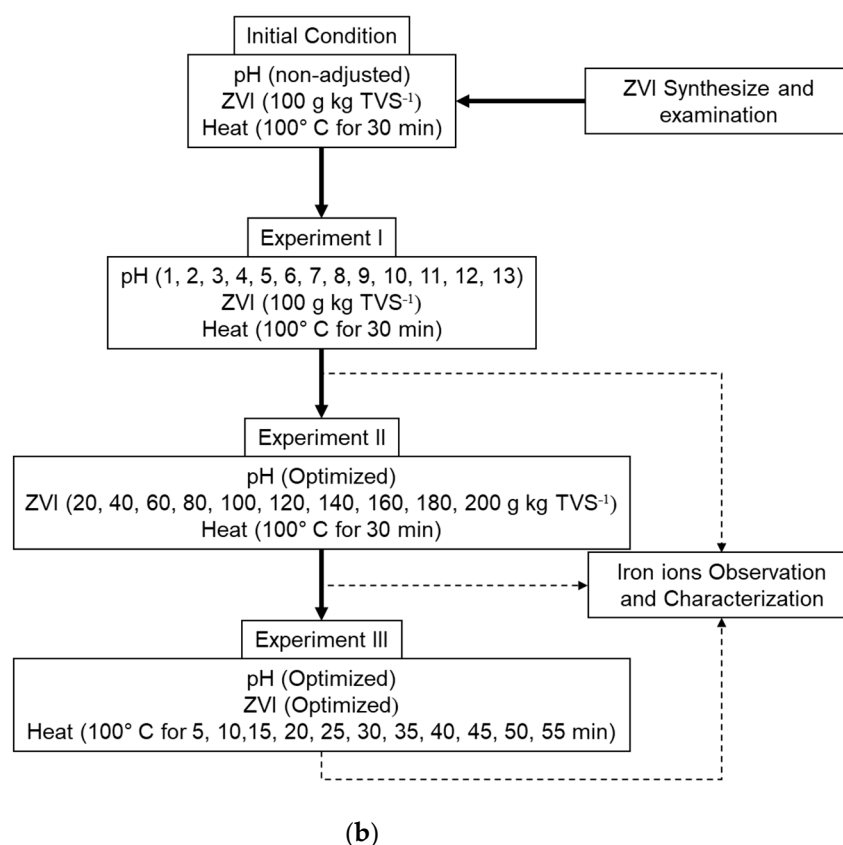


Figure 1. Design of (a) reactor, and (b) experiment in this study. (1) Effluent tank; (2) effluent outlet; (3) influent inlet; (4) AD tank; (5) pH probe; (6) gas outlet; (7) gas tank; (8) gas measurement; (9) gas chromatography machine; and (10) data collector and analyzer.

2.3. Zero-Valent Iron Preparation

Steel wool (Bonstar, Thailand) was utilized as raw material for zero-valent iron preparation. Synthesis of ZVI was conducted based on Lavine, et al. [42] and Bang, et al. [43]. Briefly, 50 g of steel wool was put in a 250 mL Erlenmeyer flask and washed with 100 mL 1% *v/v* HCl for 30 min at 150 rpm agitation. The iron was then washed with deionized water for cleaning, and, later, the residual acid and water were removed using acetone. The ZVI steel wool was dried and kept in a ziplock bag for further use.

2.4. Experimental Design

The pH adjustment and heat pretreatments were conducted simultaneously before the ZVI addition to the wastewater. The experiment was started with the initial condition of $100 \text{ g} \cdot \text{ZVI} \cdot \text{kg} \cdot \text{TVS}^{-1}$ with adjusted pH and heating for 30 min. This condition was chosen as a baseline, since the pH adjustment without heat and ZVI addition without pretreatment could produce any biogas in the preliminary test (data not shown). This condition has also been used in the industry as the standard procedure. This study had three main steps for the experiment (Figure 1b). Firstly, the pH for pretreatment was optimized by varying the pH to be 1, 2, 3, 4, 5, 6, 7, 8, 9, 10, 11, 12, and 13 by adding NaOH 5 N or H₂SO₄ 98%, while the other treatments were maintained with the normal condition. The adjusted wastewater was then heated for 30 min at 100 °C. After the pretreatment was completed, the wastewater was brought to neutral pH (pH 7), since the anaerobic process, including methanogenesis, cannot happen in low or high pH conditions. ZVI was added until the concentration reached $100 \text{ g} \cdot \text{ZVI} \cdot \text{kg} \cdot \text{TVS}^{-1}$ in all conditions. Secondly, the ZVI addition was varied from 20 to 200 $\text{g} \cdot \text{ZVI} \cdot \text{kg} \cdot \text{TVS}^{-1}$ into the wastewater after pretreatment using optimized pH conditions at 100 °C for 30 min. Lastly, the pretreatment was conducted using optimized pH with various boiling times: 0 to 55 min at 100 °C. After the pretreatment,

ZVI was added to the pretreated wastewater using the optimized concentration from the previous ZVI optimization experiment. All the anaerobic processes were conducted at room temperature (27–32 °C).

2.5. Analytical Methods

The wastewater effluent was analyzed to obtain the characteristics of COD, reducing sugars, SS, VSS, alkalinity, and VFAs. Biogas production was also analyzed daily. Furthermore, X-ray diffraction (XRD) patterns of the synthesized ZVI and the effluent from all experiments were analyzed using a Bruker D8 Advanced Diffracto Meter (Bruker, Germany). Furthermore, the morphological characteristics of ZVI before and after the experiments were also observed under a field emission scanning electron microscope (FE-SEM, Gemini 500, Zeiss, Germany). The generated biogas was also analyzed using gas chromatography (6820 GC machine, Aligent Technology, US) to measure the biogas's gas composition and methane percentage.

2.6. Mathematical Models and Kinetics

Several mathematical models for analyzing cumulative biogas production were applied in this study. Modified Gompertz (G), Logistic (L), Transference (T), and Exponential (E) models are expressed in Equations (1)–(4), respectively. These models were used numerous times in the previous study to calculate the performance parameters of the biogas cumulative production from different pretreatments and optimizations [26,35,36,44,45].

$$M = P \times \exp \left\{ -\exp \left[\frac{R_m \times e}{P} (\lambda - t) + 1 \right] \right\}, \quad (1)$$

$$M = \frac{P}{1 + \exp \left[4R_m \frac{(\lambda - t)}{P} + 2 \right]}, \quad (2)$$

$$M = P \left[1 - \exp \left(-\frac{R_m(t - \lambda)}{P} \right) \right], \quad (3)$$

$$M = P[1 - \exp(-kt)]. \quad (4)$$

Equations (1)–(3) were employed to estimate the maximum rate of biogas production (R_m , in $\text{L}\cdot\text{kg}\cdot\text{TVS}^{-1}\cdot\text{day}^{-1}$) and the duration of the lag phase (λ , in days), based on the biogas production potential (P , in $\text{L}\cdot\text{kg}\cdot\text{TVS}^{-1}$) and cumulative biogas (M , in $\text{L}\cdot\text{kg}\cdot\text{TVS}^{-1}$) at the time of the anaerobic digestion (t , in days). Meanwhile, Equation (4) calculated the hydrolysis rate coefficient (k , measured day^{-1}), which is a limiting factor for the anaerobic biodegradation.

The regression coefficient (R^2) and root mean square error (RMSE) were introduced to measure the experimental and estimated data to compare the model fitness. Equation (5) calculated the RMSE [44], where m is the number of data pairs, j is the j th value, y is the measured value, and d is the deviation between measured and predicted data.

$$\text{RMSE} = \left[\frac{1}{m} \sum_{j=1}^m \left(\frac{d_j}{y_j} \right)^2 \right]^{\frac{1}{2}}. \quad (5)$$

2.7. Data Analysis

All the experiments were conducted in triplicate. The data were shown in mean value and analyzed using t -test and ANOVA analyses using SPSS Statistical Software version 26 (IBM, USA). The Microsoft Excel Solver Tool was employed using a GRG nonlinear method in The Data Analysis tool pack to fit the experimental data with the models.

3. Results and Discussion

3.1. ZVI Characterization

Synthesis of the ZVI was conducted before the experiment of the biogas. ZVI was chosen over nanoZVI because of the potency of long-term inhibition from the ZVI and the practicality of ZVI forms [46]. The SEM and XRD observations confirmed the microstructure and iron ion compositions (Figure 2). Based on the XRD pattern, it can be confirmed that the iron wool had two primary ions. ZVI (Fe^0) has been found predominantly with a small portion of iron–carbon (Fe–C) particles based on the peaks observed in the micrograph [47]. The XDR diffractogram was observed at 2θ (Coupled Two Theta/Theta) at the wavelength of 1.54060 in the range of $10\text{--}80^\circ$ and resulted in peaks that indicated the ZVI at 45° and 65° [48]. The structure of the wool was observed to have a diameter of 0.04 mm. It is also important to note that, although the iron wool possessed a lower surface area than iron powder, the effect of the ZVI generated from the iron wool was reported to be not significantly different from the ZVI synthesized from the powder [49]. The synthesis of the iron ions is often found to not entirely form ZVI ions. As the raw material comes from the iron wool used from the steel factory, C and Fe_3O_4 are commonly used as the raw materials in this industry. It may affect the Fe–C ions found in the synthesized materials [50].

Furthermore, the small percentage of the Fe–C effect in the following process can be neglected, since it cannot give any significance to the biological process in that portion [51]. A relatively smooth surface of the substance was also observed under SEM, thus indicating a small specific surface area of the ZVI wool [47]. However, it is essential to note that the hairy macrostructure of the ZVI wool already provides a large surface area for the surface-related reaction.

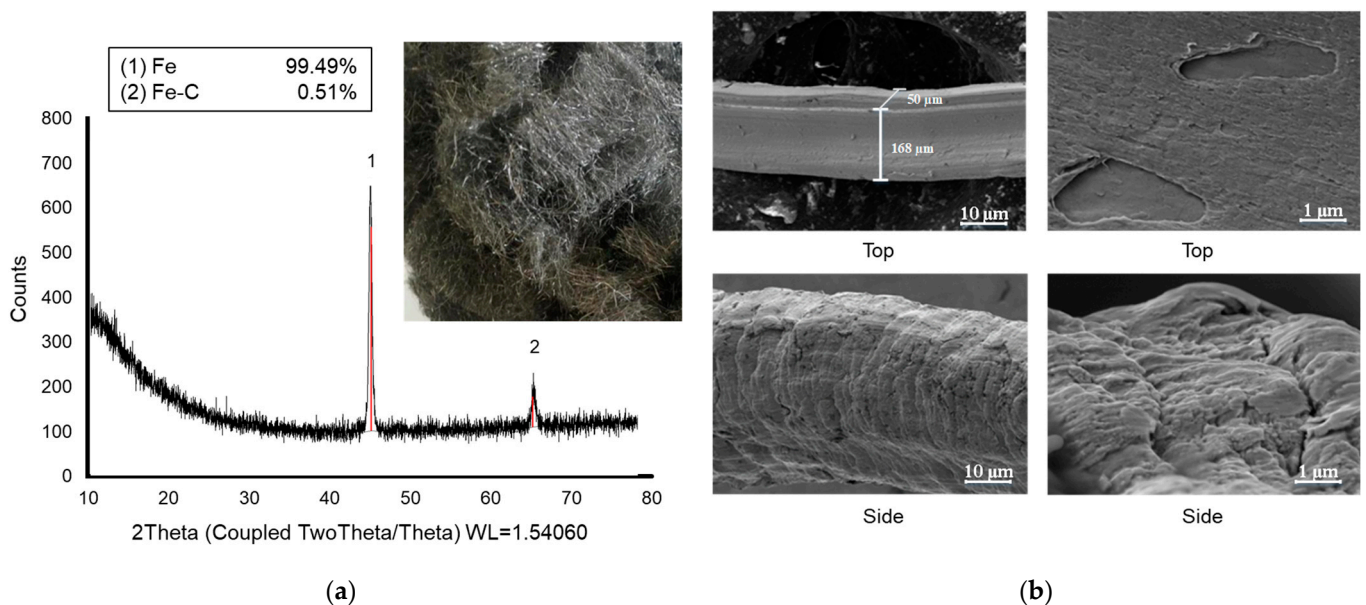


Figure 2. Characterization of ZVI synthesized from iron wool. (a) XRD patterns and (b) SEM micrograph.

3.2. Biogas Production and Composition

The cumulative biogas productions compared in different pH conditions in pretreatment, different ZVI concentrations during AD, and different heating times during the pretreatment are presented in Figure 3. The maximum cumulative biogas production was significantly different in several pretreatments. It is interesting to note that the acidic conditions during heat pretreatment produced lower biogas volumes. In contrast, the alkaline state increased biogas production more than the neutral condition. The conditions of acid, neutral, and alkaline for the pretreatment may differ depending on the lignocellulose's characteristics in the waste/wastewater as a substrate [52]. Previously, Mañunga, Barrios-Pérez, Zaiat, and Rodríguez-Victoria [10] reported that a pH of 5–5.4 was the optimum range to

create suitable substrate conditions for further digestion in cassava wastewater. However, the wastewater from the cassava industry had a higher biomass containing a high level of starchy lignocellulosic substances [53]. It is important to note that acidic conditions may help release monomeric sugars and hydrolysates from hemicellulose and cellulose in cassava pulp wastewater. However, it also potentially generates toxic substances such as furfural and hydroxymethyl furfural (HMF) [54]. Furthermore, lignin is also hardly hydrolyzed in acidic conditions and may condensate and precipitate [55]. On the other hand, the alkaline state, through solvation and saponification, induces depolymerization and cleavage of the lignin-carbohydrate bond to provide an accessible substance for hydrolysis enzymes [56]. Similar studies using cassava pulp wastewater showed the change of the substrate's composition after the pretreatment of pH and heat together with the ZVI addition. It has been reported that the alkaline pretreatment had a significant impact on the removal of lignin (24–38%) and hemicellulose (48–58%) to the forms that could be easily converted into fatty acids for methanogenesis processes [13].

In the ZVI experiment, a moderate concentration of ZVI was found to enhance biogas production optimally. In contrast, excess concentrations had a lower effect on biogas production than moderate ones. However, a low ZVI concentration also increased the biogas production compared to the control condition. The low ZVI concentration could not be adequately sufficient for the whole enhancement in the system. At the same time, inhibition due to excess ZVI and its derivatives may explain the reduction of the result in higher ZVI concentrations. It was in line with the outcome of Puyol, et al. [57], which showed that excess ZVI reduced methane production from the AD. Similarly, a previous study using similar wastewater showed that the optimum condition was 50–60 g·ZVI·kg·TVS⁻¹ [48]. This phenomenon may be related to the high accumulation of Fe²⁺ and Fe³⁺ that inhibit the process of methanogenesis, as the excess attachment may be found in the methanogenesis with the iron ions [46]. Another possible mechanism is the competition for free electrons between Fe₃O₄ that resulted from the ZVI oxidation and methanogens in the excess applied concentration [58].

Thirty-five minutes was the optimum time for boiling pretreatment for the heating experiment. It was slightly higher than 30 and 40–45 min of heating at 100 °C (Figure 3c). As with the alkaline pretreatment, the high temperature condition was proposed to break the lignin bonds and provide holocellulose fractions for further degradation processes [59]. Previously, different heating times were reported from heat pretreatment studies. Thirty minutes was reported to be suitable for cassava pulp at 100 °C [48], 180 °C, and 60 min for cattle manure, corn silage, and sugar beet pulp residues [60], as well as 157.84 °C for 20.15 min to pretreat cassava residues [11]. Interestingly, a more extended heating period resulted in slightly lower biogas production. Longer treatment times may also cause higher energy consumption and thus negatively affected the pretreatments' feasibility [61]. It is also important to notice that there was a dramatical increase in methane production after increasing the heating time from 25 min to 35 min (Figure 3c). This situation indicates that 35 min might be the threshold of specific heat required to break the lignocellulose structures and release the monomeric sugars in the complex of hardly degradable cassava wastewater. Previously, the dramatic increase in methane production after a small increase in the heating period has been observed by conventional and microwave pretreatments [62–64]. The lower reaction time in heat was reported to produce minor damage in the structure of cellulose and lignocellulose, while slightly different time, temperature, and catalyst concentrations resulted in high differences in the biogas production [65].

Overall, each pretreatment and ZVI addition increased the biogas production from the standard or previous experiment condition. This result showed that each pretreatment is vital in preparing the wastewater to enter the AD phase. Meanwhile, adding ZVI was also proven to enhance biogas generation. This was contrary to Aruwajoye et al., who showed that the increase in H₂SO₄ in pretreatment would still be effective, even without any heating time optimization [66]. It has been reported that increasing the acid concentration in sorghum pretreatment did not optimally prepare the substrate for the other

process when it was not coupled with thermal conditions [67]. Based on the net energy calculation that was adopted from Liu et al. [68], it has been found that the application of the combination of optimized pH and heating time with ZVI concentration resulted in a positive net energy of $178 \text{ MJ}\cdot\text{t}^{-1}$ compared to the negative energy production in the control condition ($-225 \text{ MJ}\cdot\text{t}^{-1}$).

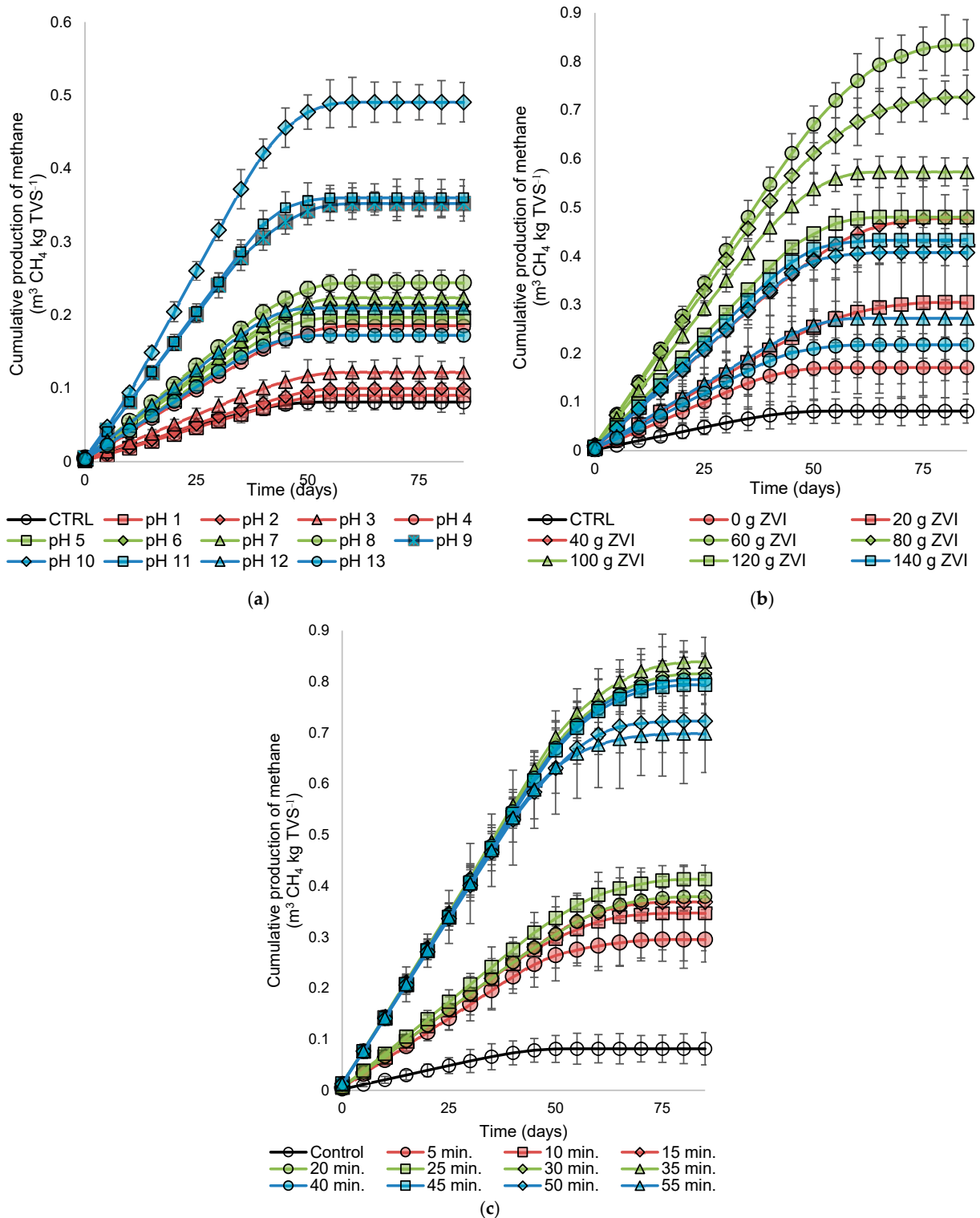


Figure 3. Cumulative methane yield from three different experiments. (a) Pretreatment using different pH, (b) ZVI addition into AD, and (c) heating times in pretreatment.

The methane (CH₄) percentage in the total biogas was also higher along with the pH gradient in the first experiment (Figure 4). However, the second and third experiments did not significantly change the percentage of methane production. Acid pretreatment often resulted in the effective degradation of the lignin and hemicellulose. However, acid pretreatment may generate toxic substances such as furfural and HMF [11]. This situation can lead to fermentation with a high percentage of CO₂ as the intermediate form, since the methanogens that are supposed to convert CO₂ and H₂ were inhibited by the furfural and HMF [67].

It is also worth noting that applying an optimal ZVI concentration followed by an optimum heating temperature for pretreatment resulted in a higher CH₄ portion. It indicates that the biogas quality's main focus was the pH adjustment in the heat pretreatment. However, ZVI and heating time still played an essential role in generating biogas that accumulated sufficient CH₄ amounts. It has been previously described that the optimization of the pretreatment conditions may result in the biogas quality being indicated by the CH₄ percentage, and, in prolonged production, this resulted in a higher amount of biogas production [69].

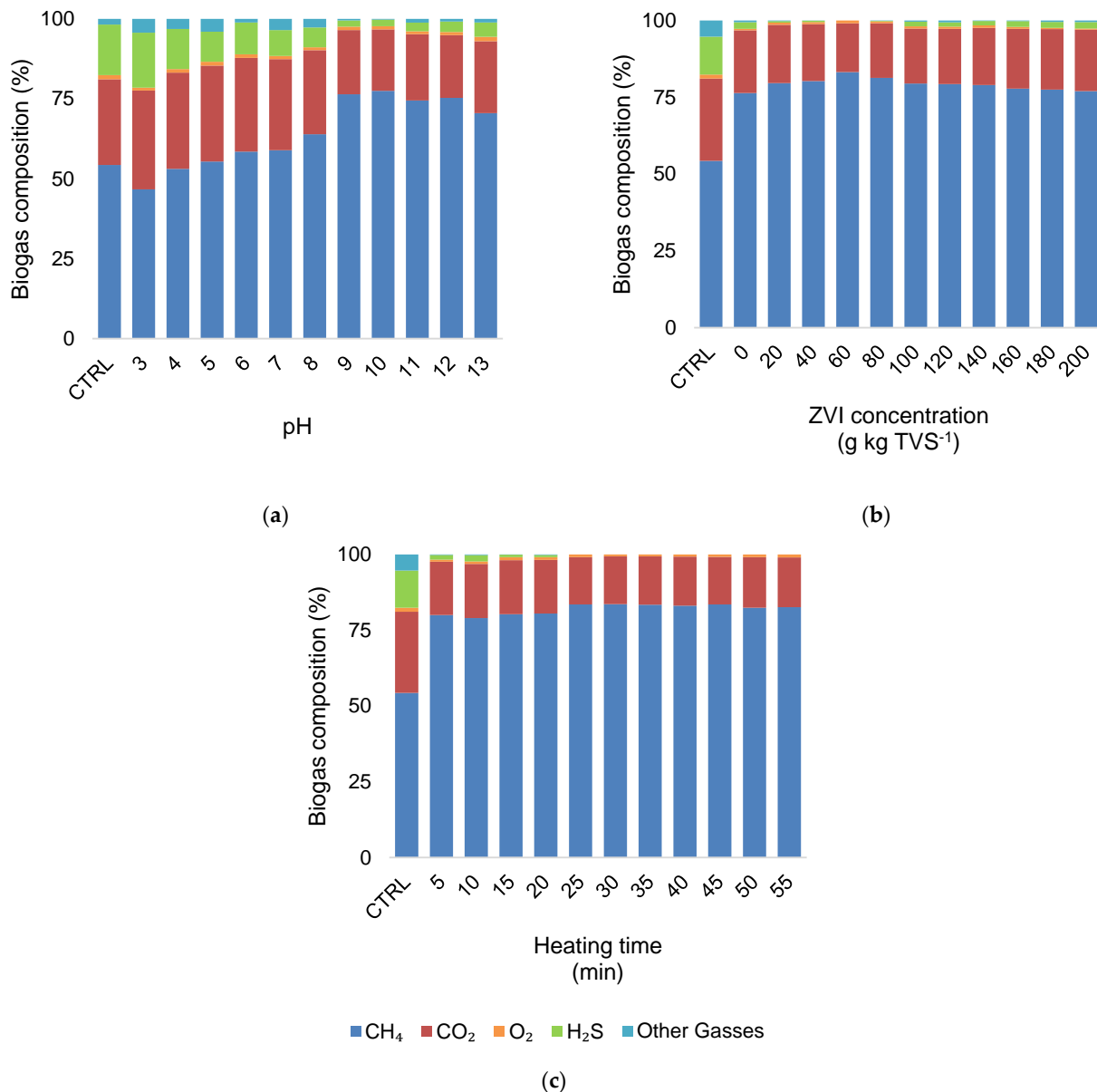
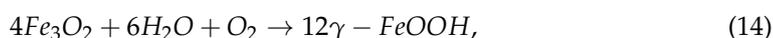
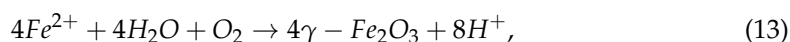
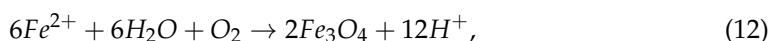
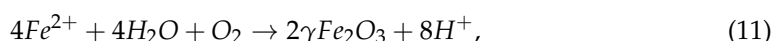
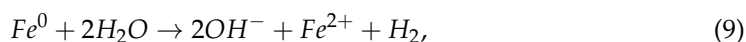
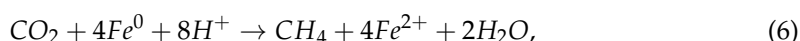


Figure 4. Biogas composition generated from different experiments. (a) The pH adjustment in pretreatment, (b) ZVI addition in AD, and (c) heating time adjustment in pretreatment.

3.3. Substrate and ZVI Utilizations

The removal efficiencies of critical parameters in the substrate showed that a proper pH condition (pH 10) in the heat pretreatment significantly increased the COD removal, while the VSS, SS, and reducing sugars underwent moderate removal efficiencies compared to other pH conditions (Figure 5a). The acid and alkaline conditions had high removals of reducing sugars, while the others were still in between, thus indicating that the breaking bonds of the lignocellulose in cassava effluent were successfully conducted during the acid–alkaline conditions [29]. The higher reducing sugar removals in the acid conditions were due to the better performance of cellulose reduction in the acid conditions. They prepared the cellulose and its derivatives for enzyme hydrolysis more efficiently than the alkaline pretreatment, although the lignin was not entirely hydrolyzed in the acid condition [70]. Overall, the solubilization of organic matter performed better in the alkaline than in the acid conditions [13].

However, the removal efficiencies were optimum in the 60 g·kg·TVS⁻¹ addition of ZVI. Interestingly, a heating period longer than the optimum (35 min) resulted in lower SS removal efficiency. Here, the acid and alkaline conditions in the heat pretreatment mainly focused on breaking the strong lignin and hemicellulose bonds in the hardly degradable substrate [29]. It provided a high carbon source from the reducing sugars for acidogenesis and acetogenesis. Meanwhile, the ZVI targeted the later stage of methane production: methanogenesis. Although the positive effects of ZVI have been recorded during hydrolysis–acidogenesis phases [71], the primary function of ZVI was also pointed out as an electron donor by corrosion reaction to produce hydrogen gas and co-factor for several vital enzymes for facilitating fermentation during methanogenesis processes [20,72]. In this study, the high removal of COD and the low VFAs concentration at the end of experiment II (Figure 5a) indicated that the excess concentration of ZVI enhanced the hydrolysis–acetogenesis processes but did not inhibit the conversion of methane generation at the last stage. This also indicated that the excess ZVI only appeared to be an additional assistance in the formation of VFA by alleviating the acidification, while the main role of the ZVI and its derivatives was in the enzyme activity and metabolism of the methanogens, thus reducing the odorous gasses (sulfur derivatives) and leading to the degradation of refractory substances [32].



The fate of iron ions in the AD system was examined after the biogas generation process. It has been shown that the Fe⁰ ions were converted into Fe³⁺ and Fe²⁺, with

only less than 10% remaining in the Fe⁰ form (Figure 5b). The records of iron ions at the end of the period were found to be Fe³⁺ (FeOOH, FeS₂, Fe₂O₃, Fe₃O₄) and Fe²⁺ (FeO, FeCO₃, Fe(OH)₂). In the ZVI application in the AD, the corrosion reaction was reported as the typical reaction (Equations (6) and (7)). Several reactions, including acidification (Equation (8)), also formed different states of iron ions in the system. ZVI was oxidized to Fe²⁺ under anaerobic conditions and affected methanogens, enhanced enzyme activity, and triggered a large percentage of protein in electronic power steering (EPS) [73].

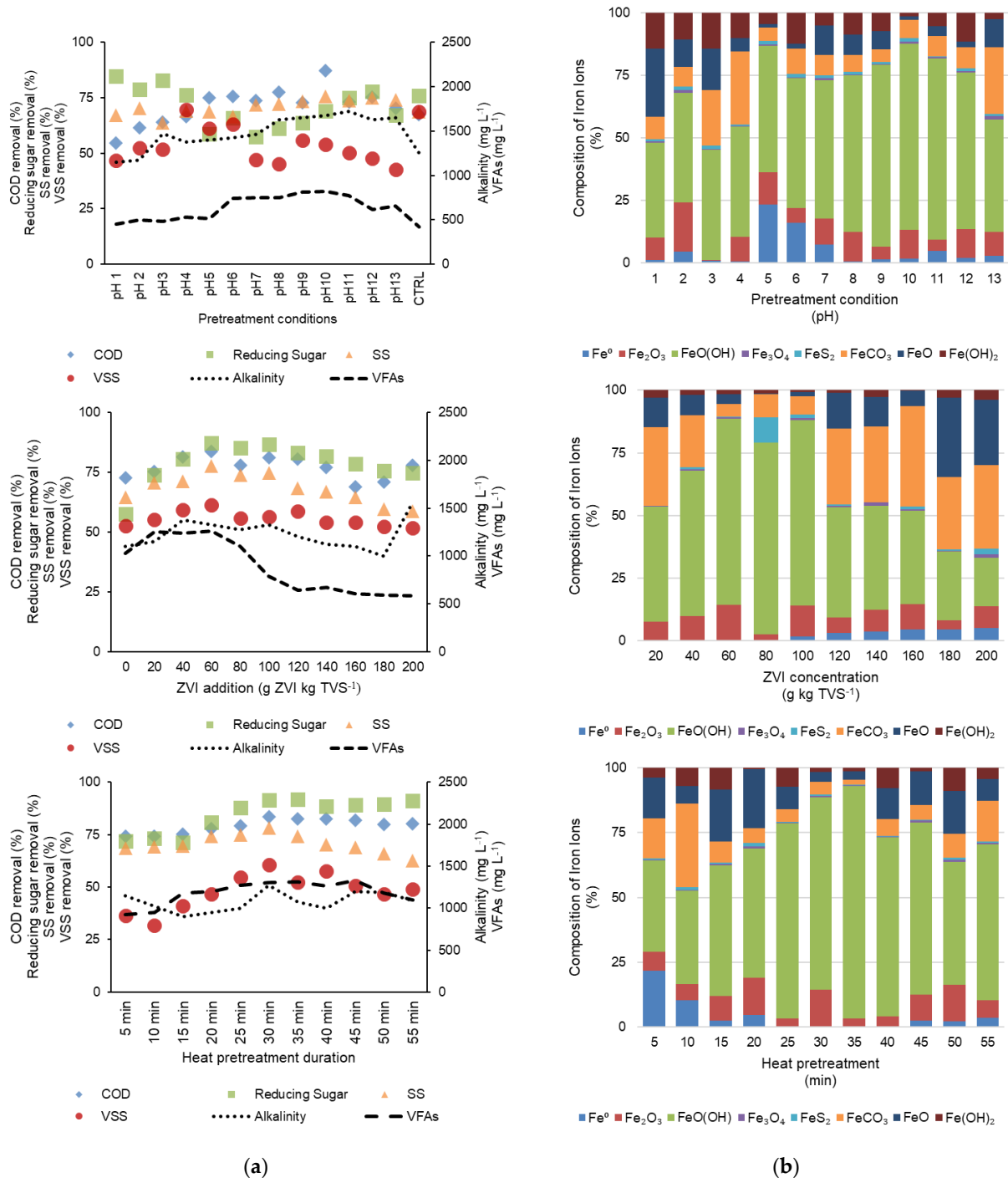


Figure 5. The effluent characteristics after AD in different pretreatment and additive adjustments. (a) effluent characteristics regarding methane production and wastewater parameters, and (b) iron ion compositions from the ZVI addition.

It has also been reported that Fe^0 can directly react with water and oxygen to form Fe^{3+} (Equations (11)–(13)) in the form of Fe_2O_3 [74]. The previous study also mentioned that, due to the large surface of the ZVI, Fe^{3+} could be found in the forms of FeOOH and Fe_3O_4 after a direct reaction with water and oxygen [73]. However, Fe^{3+} can be utilized by iron-reducing bacteria as an electron acceptor in degrading organic matter by converting Fe^{3+} into Fe^{2+} [75]. It is also interesting to note that the free electron can still be produced by oxidizing Fe^{2+} into Fe^{3+} , thus releasing more H^+ into the system (Equations (11)–(13)) that is later oxidized into maghemite (FeOOH) as the end products (Equations (14) and (15)) [76]. In this study, the organic matter-assisted degradation through the ZVI scenario may have occurred less, as the degradation of organic matter was already optimized by the pretreatments. It is also important to note that Fe_3O_4 potentially inhibited methanogenesis, although it dramatically promotes hydrolysis and acidification [58]. Similarly, the treatments that produced high biogas production (pH 10, ZVI 60 g·kg·TVS⁻¹, and 35 min of heating) showed a high percentage of Fe^{3+} (FeOOH) and a low percentage of Fe^{2+} (FeCO_3) compared to the treatments that showed lower biogas production. As the effluent collected at biogas production was negligible, the activity of the Fe ions was assumed to reach the final forms. Similarly, Ren, et al. [77] stated that Fe^{2+} was a reactive form of Fe ions and thus can still enhance the AD process, while Fe^{3+} was reported to be less beneficial to AD, as the state had already reached the end form.

Furthermore, the SEM observation (Figure S1) revealed that aggregated sample formation was observed in the optimum conditions. In contrast, a relatively smooth surface was observed in the low performance conditions. Zhu, et al. [78] reported that the optimum concentration of ZVI resulted in a high occurrence of granule structures to avoid the impacts of high VFA concentrations. The granule, rough-surface grains after the addition of ZVI can be caused by the disruption of aggregated sludge particles that enhance the performance of digestion and the ZVI that underwent oxidation to become Fe^{3+} and Fe^{2+} [76,79]. Based on these results, it can be concluded that the addition of ZVI could directly enhance the methane production through several direct mechanisms, while the derivatives of ZVI were formed, such as magnetite, ferrous, and ferric ions.

3.4. Models for Biogas Production

The application of several mathematical models, namely, the *Modified Gompertz equation* (G), *Logistic function equation* (L), *Transference function equation* (T), and *Exponential* (E), showed the overall agreement between the models results (Tables S1–S4) and the experimental data (Figure 6a–c). By comparing the performance models, the fittest models were obtained using the *Logistic Function Equation* (L) and *Modified Gompertz equation* (G) models, which achieved significantly higher regression of coefficient values in three experiment data (Figure 6d). These results are in line with the previous studies that found the two models (L and G) were the most suitable models for evaluating the pretreatment effects on kinetics parameters such as lag phase (λ) and biogas production rate (R_m) [35,80].

Interestingly, the Logistic function model was significantly different from other models in the third experiment based on the R^2 values comparison, and the typical exponential model using only one coefficient (k) was the lowest-fitted model ($R^2 < 0.97$). The first-order exponential model is often used due to its simplicity since it involves only one coefficient and is thus more suitable for comparing kinetics values [81]. However, it is often found to not be sensitive to the variation from pretreatment results [82]. Thus, it is not recommended for the complex combinations of pretreatments and enhancement by additives that were performed in this study. In high-sensitivity optimization, the models' sensitivity can determine the significant difference in the output. The Modified Gompertz model, although more frequently used and often able to satisfy the results in biogas accumulation calculation [83,84], was found below the logistic function in this study. Donoso-Bravo, Pérez-Elvira, and Fdz-Polanco [82] proposed that pretreatments and enhancement during AD may result in slightly different biogas production and may affect the Modified Gompertz's lower sensitivity over the Logistic model.

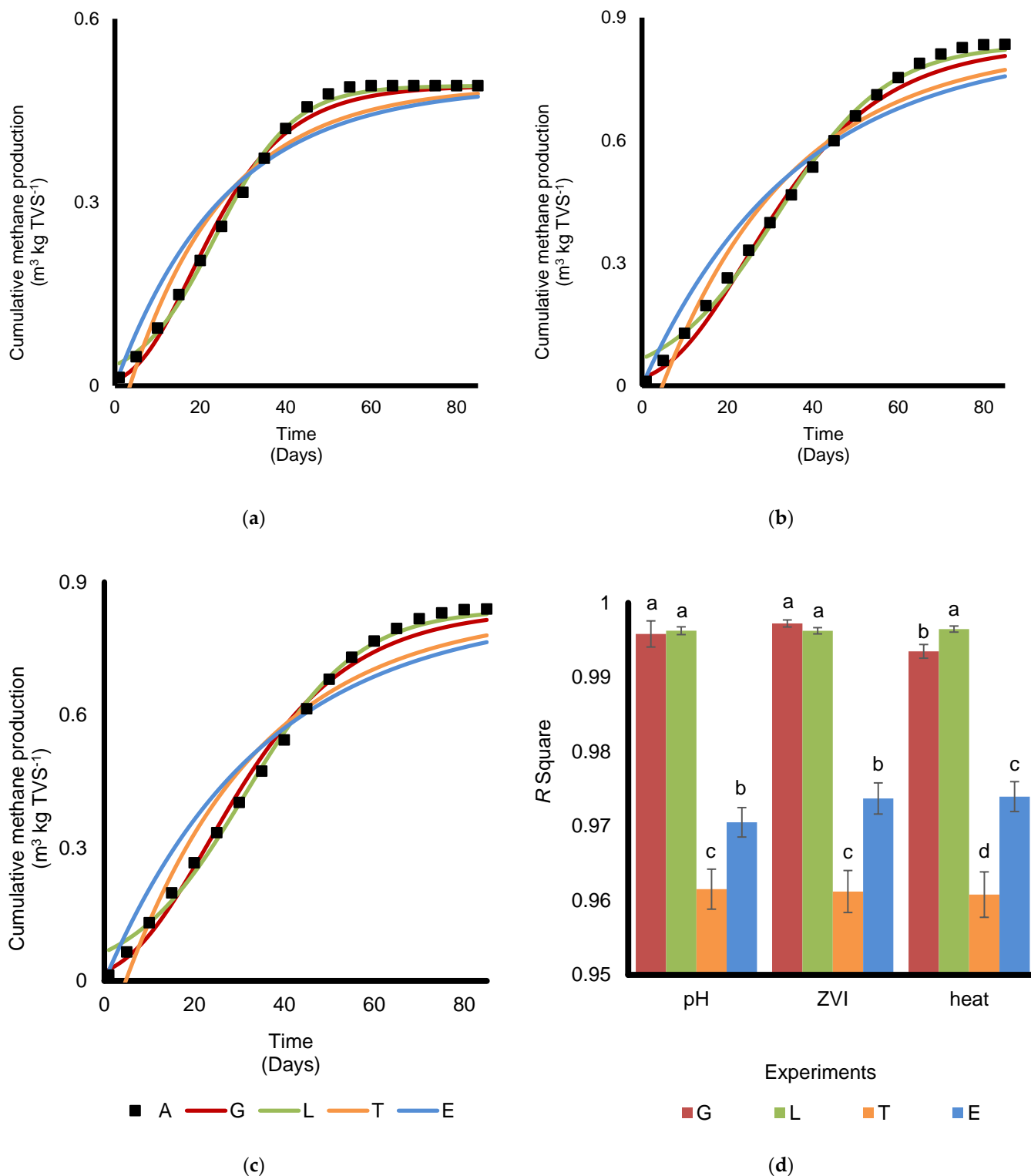


Figure 6. Model fit with methane yield in different experiments with the most satisfied result from each experiment. (a) The pH optimization with the actual value of pH ten treatment, (b) ZVI addition with the actual value of 60 g·kg·TVS⁻¹, (c) heating time optimization in the actual value of 35 min, and (d) regression coefficient (R²) of the applied models in different pretreatments (different letters show different significant differences).

Kinetics parameters were calculated from the three experiments (Table 2). The pH experiment revealed the λ to be 5.011, 5.644, and 3.503 days, using the G, L, and T models,

respectively. Interestingly, the values increased in the ZVI experiments (6.199, 5.857, and 4.771 days in the G, L, and T models, respectively) and later decreased in the heat experiments (5.245, 6.056, and 4.744 days in the G, L, and T models, respectively). This study’s calculated lag phase period was relatively moderate compared to the previous studies’ results. Deepanraj, et al. [85] reported a lag phase of 1.5 to 2.8 days in food waste processes, while Pardilhó, et al. [86] calculated the value of 11 to 17.2 days in microalgae biomass. The different lag phases correspond to the hydrolysis processes at the early stage of AD and the adaptation or acclimatization from the microorganisms in the system [80,86].

In contrast to other reports, the biogas production rate (R_m , m^3 biogas $kg \cdot TVS^{-1} \cdot day^{-1}$) showed a constant increase of the values from the first to the last experiment sets. In the Modified Gompertz model, the R_m was found to be 0.014, 0.017, and 0.018 m^3 of biogas $kg \cdot TVS^{-1} \cdot day^{-1}$ in three consecutive experiments. In the Logistic model, the R_m were 0.014, 0.016, and 0.017 m^3 of biogas $kg \cdot TVS^{-1} \cdot day^{-1}$ in the pH, ZVI, and heat experiments, respectively. Again, these results are lower than the average than most of the R_m values reported previously, which ranged from 0.037–0.587 $g \cdot L$ of biogas $kg \cdot TVS^{-1} \cdot day^{-1}$ [35,86,87]. Similar to the lag phase, the R_m is also an important parameter to determine the volume of biogas. Thus, the rates are related to the substrate characteristics and seeds’ adaptability in the AD process [35]. The low production and rate of biogas production can vary because of the substrates and seeds that are applied into the AD. The results of the methane production (P) in this study were relatively higher than several substrates that have been previously studied, such as organic fraction municipal solid waste and biological sludge ($P = 0.544.3 m^3 \cdot CH_4 \cdot kg \cdot TVS^{-1}$) [88], cassava pulp ($P = 0.324 \pm 5 m^3 \cdot kg \cdot TVS^{-1}$) [13], weeds ($P = 0.024 m^3 \cdot kg \cdot TVS^{-1}$) [27], and rice straw with corn stalk ($P = 0.39 m^3 \cdot kg \cdot TVS^{-1}$) [89].

Table 2. Kinetics parameters from four different models of the optimum conditions in three experiments (pH adjustment, ZVI addition, and heating time).

Models	Parameters	Exp. I (pH 10)	Exp. II (60 g·ZVI·kg·TVS ⁻¹)	Exp. III (35 min Heating)
Modified Gompertz	<i>P</i>	0.491	0.834	0.839
	<i>R_m</i>	0.014	0.017	0.018
	λ	5.011	6.199	5.352
	<i>R</i> ²	0.997	0.997	0.993
Logistic Function	<i>P</i>	0.491	0.834	0.839
	<i>R_m</i>	0.014	0.016	0.017
	λ	5.644	5.857	6.056
	<i>R</i> ²	0.997	0.996	0.997
Transference Function	<i>P</i>	0.491	0.834	0.839
	<i>R_m</i>	0.022	0.027	0.028
	λ	3.503	4.771	4.744
	<i>R</i> ²	0.959	0.959	0.958
Exponential Function	<i>P</i>	0.491	0.834	0.839
	<i>k</i>	0.039	0.028	0.028
	<i>R</i> ²	0.969	0.973	0.972

The correlation tests from all the kinetics parameters from Logistic and Modified Gompertz, which were the most fitted models with effluent characteristics, were also conducted (Table S5). They revealed a moderate-to-strong relationship between the concentration of FeOOH at the end of the AD and the kinetics parameters (P and R_m), with the R^2 value ranging from 0.958 to 0.997. This result also strengthened the complete process of ZVI oxidation into the end form of FeOOH [76]. While other intermediate ions and effluent characteristics also possess significant deviations and thus cannot be correlated with the biogas generation kinetics, end products of additives usually depict the kinetics process of the AD process [90,91]. However, the lack of correlation of the λ in several experiments was acceptable and negligible, since the adaptation of the microbial community in the AD

can be different depending on the substrate and seeds composition as the main factors for the lag phase [80,86].

The combination of pH adjustment in the pretreatment with the ZVI addition showed increased biogas production and improved methane content. Several key findings were as follows:

1. The alkaline condition showed effective performance in the heat pretreatment for cassava pulp wastewater. Although the acid showed higher organic matter removal, the biogas generation was better in the alkaline–heat pretreatment.
2. Synthesized ZVI was successfully applied in the AD. It was made from the affordable and abundant raw material iron wool. The Fe^0 oxidation reached the end product of FeOOH (Fe^{3+}), which was depicted by the large portion of these iron forms at the end of biogas generation.
3. Several models were used to calculate the kinetics parameters of the papers. It can be seen that the Modified Gompertz and Logistic models fit the data more than the Transference Function model, with a slightly better performance of the Logistic model. A correlation between the kinetics parameters from the suitable models was also found. The R_m and maximum biomass potential correlated with the effluent's FeOOH .

Although these findings are novel in the anaerobic digestion of cassava pulp wastewater, several limitations and further development prospects can still be pointed out.

1. The optimization using three experiment steps may still be improved to determine the exact time, pH, and ZVI concentrations in other approaches to obtain accurate numbers for each treatment [11,38]. Several previous studies regarding biogas optimization that involved several parameters had used factorial or response surface method experimental designs to obtain more detail levels of pH, durations of heating, and concentrations of ZVI. The mentioned experimental designs can also be explained further using principal component analysis (PCA), where the relationship between each dataset can be observed in detail.
2. The claim of correlation of the P and R_m with FeOOH concentration can be further analyzed and tested in numerous experiments. It can also help to better understand the mechanisms and efficiency of the AD system [76].
3. SS and VSS removals efficiencies were still moderate. Thus, different processes must be performed before the effluent can be recycled or released into the environment. Several studies have performed better using other substrates [24,45]. In future investigations, the efficiency of removals shall be deliberated in the overall output from the addition of pretreatment and additives.
4. The modification of pretreatments and the addition of ZVI may result in switches of the microbial community in the AD system. The switch may also be important to be observed and determined in order to determine the sustainability of the recirculate effluent as seeds with regard to the quality of the generated biogas [5].

4. Conclusions

Optimizing heat pretreatment in several pHs combined with ZVI addition has been conducted. It has been found that the most optimum condition was a pH of 10 for 100 °C for 35 min and the addition of 60 g·ZVI·kg·TVS⁻¹ of wastewater. Most irons at the end of AD were found in the form of FeOOH (Fe^{3+}). Of four different mathematical models for cumulative biogas production, the Logistic model was found as the fittest model. It was slightly better than the Modified Gompertz model, which is usually applied in a similar system. The concentration of Fe^{3+} was also found to correlate with the kinetics parameters from selected mathematical models, which were maximum biogas potential and biogas production rate.

Pretreatments and the addition of ZVI in the cassava pulp wastewater also showed an improvement in the net energy of 178 MJ·t⁻¹ from –225 MJ·t⁻¹. It is also important to note that the high energy net improvement may also result in higher cost reduction and

efficient performance in the larger scale of application. Overall, this study's result is novel and essential with regard to establishing the mathematical models for combining additives and pretreatments. It may also be applied for upscaling the bioprocess of cassava pulp wastewater as a biogas production substrate.

Supplementary Materials: The following supporting information can be downloaded at: <https://www.mdpi.com/article/10.3390/fermentation9070622/s1>, Figure S1: SEM observation from different treatments and pretreatments; Table S1: Kinetics parameters of pH, ZVI, and heating period experiments from four mathematical models for biogas production from Modified Gompertz Model; Table S2: Kinetics parameters of pH, ZVI, and heating period experiments from four mathematical models for biogas production from Logistic Model; Table S3: Kinetics parameters of pH, ZVI, and heating period experiments from four mathematical models for biogas production from Transference Model; Table S4: Kinetics parameters of pH, ZVI, and heating period experiments from four mathematical models for biogas production from Exponential Model; Table S5: Pearson's correlation test results from several kinetics parameters and iron ions states in effluent.

Author Contributions: Conceptualization, N.B. and U.Y.; methodology, U.Y.; software, M.P.; validation, N.B., U.Y. and M.P.; formal analysis, M.P.; investigation, U.Y.; resources, N.B.; data curation, M.P.; writing—original draft preparation, M.P.; writing—review and editing, N.B.; visualization, M.P.; supervision, N.B.; project administration, U.Y.; funding acquisition, N.B. All authors have read and agreed to the published version of the manuscript.

Funding: This research received no external funding.

Institutional Review Board Statement: Not applicable.

Informed Consent Statement: Not applicable.

Data Availability Statement: The data presented in this study are available.

Conflicts of Interest: The authors declare no conflict of interest.

References

1. Wattanasilp, C.; Songprakorp, R.; Nopharatana, A.; Khompatraporn, C. Techno-Cost-Benefit Analysis of Biogas Production from Industrial Cassava Starch Wastewater in Thailand for Optimal Utilization with Energy Storage. *Energies* **2021**, *14*, 416. [CrossRef]
2. Lin, H.; Borrion, A.; da Fonseca-Zang, W.A.; Zang, J.W.; Leandro, W.M.; Campos, L.C. Life cycle assessment of a biogas system for cassava processing in Brazil to close the loop in the water-waste-energy-food nexus. *J. Clean. Prod.* **2021**, *299*, 126861. [CrossRef]
3. dos Santos, A.L.M.; Castro, A.L.S.; Salomon, K.R.; de Souza, T.S.O.; Vich, D.V. Global research trends on anaerobic digestion and biogas production from cassava wastewater: A bibliometric analysis. *J. Chem. Technol. Biotechnol.* **2022**, *97*, 1379–1389. [CrossRef]
4. Cruz, I.A.; Santos Andrade, L.R.; Bharagava, R.N.; Nadda, A.K.; Bilal, M.; Figueiredo, R.T.; Romanholo Ferreira, L.F. Valorization of cassava residues for biogas production in Brazil based on the circular economy: An updated and comprehensive review. *Clean. Eng. Technol.* **2021**, *4*, 100196. [CrossRef]
5. Mirmohamadsadeghi, S.; Karimi, K.; Azarbajjani, R.; Parsa Yeganeh, L.; Angelidaki, I.; Nizami, A.-S.; Bhat, R.; Dashora, K.; Vijay, V.K.; Aghbashlo, M.; et al. Pretreatment of lignocelluloses for enhanced biogas production: A review on influencing mechanisms and the importance of microbial diversity. *Renew. Sustain. Energy Rev.* **2021**, *135*, 110173. [CrossRef]
6. Gunes, B.; Stokes, J.; Davis, P.; Connolly, C.; Lawler, J. Pre-treatments to enhance biogas yield and quality from anaerobic digestion of whiskey distillery and brewery wastes: A review. *Renew. Sustain. Energy Rev.* **2019**, *113*, 109281. [CrossRef]
7. Zhang, M.; Xie, L.; Yin, Z.; Khanal, S.K.; Zhou, Q. Biorefinery approach for cassava-based industrial wastes: Current status and opportunities. *Bioresour. Technol.* **2016**, *215*, 50–62. [CrossRef]
8. Okudoh, V.; Trois, C.; Workneh, T.; Schmidt, S. The potential of cassava biomass and applicable technologies for sustainable biogas production in South Africa: A review. *Renew. Sustain. Energy Rev.* **2014**, *39*, 1035–1052. [CrossRef]
9. Toreci, I.; Droste, R.L.; Kennedy, K.J. Mesophilic Anaerobic Digestion with High-Temperature Microwave Pretreatment and Importance of Inoculum Acclimation. *Water Environ. Res.* **2011**, *83*, 549–559. [CrossRef]
10. Mañunga, T.; Barrios-Pérez, J.D.; Zaiat, M.; Rodríguez-Victoria, J.A. Evaluation of pretreatment methods and initial pH on mixed inoculum for fermentative hydrogen production from cassava wastewater. *Biofuels* **2022**, *13*, 301–308. [CrossRef]
11. Zhang, Q.; Tang, L.; Zhang, J.; Mao, Z.; Jiang, L. Optimization of thermal-dilute sulfuric acid pretreatment for enhancement of methane production from cassava residues. *Bioresour. Technol.* **2011**, *102*, 3958–3965. [CrossRef] [PubMed]
12. Lyu, H.; Zhang, J.; Zhou, J.; Lv, C.; Geng, Z. The byproduct-organic acids strengthened pretreatment of cassava straw: Optimization and kinetic study. *Bioresour. Technol.* **2019**, *290*, 121756. [CrossRef]
13. Lomwongsopon, P.; Aramrueang, N. Mild chemical pretreatment of cassava pulp for enhancing high-load anaerobic digestion. *Bioresour. Technol. Rep.* **2022**, *17*, 100896. [CrossRef]

14. Guo, Q.; Majeed, S.; Xu, R.; Zhang, K.; Kakade, A.; Khan, A.; Hafeez, F.Y.; Mao, C.; Liu, P.; Li, X. Heavy metals interact with the microbial community and affect biogas production in anaerobic digestion: A review. *J. Environ. Manag.* **2019**, *240*, 266–272. [[CrossRef](#)] [[PubMed](#)]
15. Wandera, S.M.; Qiao, W.; Algapani, D.E.; Bi, S.; Yin, D.; Qi, X.; Liu, Y.; Dach, J.; Dong, R. Searching for possibilities to improve the performance of full scale agricultural biogas plants. *Renew. Energy* **2018**, *116*, 720–727. [[CrossRef](#)]
16. Hoelzle, R.D.; Virdis, B.; Batstone, D.J. Regulation mechanisms in mixed and pure culture microbial fermentation. *Biotechnol. Bioeng.* **2014**, *111*, 2139–2154. [[CrossRef](#)]
17. Ho, D.; Jensen, P.; Batstone, D. Effects of Temperature and Hydraulic Retention Time on Acetotrophic Pathways and Performance in High-Rate Sludge Digestion. *Environ. Sci. Technol.* **2014**, *48*, 6468–6476. [[CrossRef](#)] [[PubMed](#)]
18. Ye, M.; Liu, J.; Ma, C.; Li, Y.-Y.; Zou, L.; Qian, G.; Xu, Z.P. Improving the stability and efficiency of anaerobic digestion of food waste using additives: A critical review. *J. Clean. Prod.* **2018**, *192*, 316–326. [[CrossRef](#)]
19. Su, L.; Zhen, G.; Zhang, L.; Zhao, Y.; Niu, D.; Chai, X. The use of the core-shell structure of zero-valent iron nanoparticles (NZVI) for long-term removal of sulphide in sludge during anaerobic digestion. *Environ. Sci. Process. Impacts* **2015**, *17*, 2013–2021. [[CrossRef](#)]
20. Wu, D.; Zheng, S.; Ding, A.; Sun, G.; Yang, M. Performance of a zero valent iron-based anaerobic system in swine wastewater treatment. *J. Hazard. Mater.* **2015**, *286*, 1–6. [[CrossRef](#)]
21. Zhang, S.; Ren, Y.; Ma, X.; Guan, W.; Gao, M.; Li, Y.-Y.; Wang, Q.; Wu, C. Effect of zero-valent iron addition on the biogas fermentation of food waste after anaerobic preservation. *J. Environ. Chem. Eng.* **2021**, *9*, 106013. [[CrossRef](#)]
22. Gundoshmian, T.M.; Ahmadi-Pirlou, M. Increasing biogas and methane yield by adding sewage sludge and zero-valent iron nanoparticles during the single-stage anaerobic digestion with municipal solid waste. *Int. J. Energy Res.* **2022**, *46*, 20611–20623. [[CrossRef](#)]
23. Domrongpokkaphan, V.; Phalakornkule, C.; Khemkhao, M. In-situ methane enrichment of biogas from anaerobic digestion of palm oil mill effluent by addition of zero valent iron (ZVI). *Int. J. Hydrog. Energy* **2021**, *46*, 30976–30987. [[CrossRef](#)]
24. Ugwu, S.N.; Enweremadu, C.C. Enhancement of biogas production process from biomass wastes using iron-based additives: Types, impacts, and implications. *Energy Sources Part A Recovery Util. Environ. Eff.* **2022**, *44*, 4458–4480. [[CrossRef](#)]
25. Zhang, Y.; Feng, Y.; Quan, X. Zero-valent iron enhanced methanogenic activity in anaerobic digestion of waste activated sludge after heat and alkali pretreatment. *Waste Manag.* **2015**, *38*, 297–302. [[CrossRef](#)] [[PubMed](#)]
26. Sarto, S.; Hildayati, R.; Syaichurrozi, I. Effect of chemical pretreatment using sulfuric acid on biogas production from water hyacinth and kinetics. *Renew. Energy* **2019**, *132*, 335–350. [[CrossRef](#)]
27. Syaichurrozi, I.; Villta, P.K.; Nabilah, N.; Rusdi, R. Effect of sulfuric acid pretreatment on biogas production from *Salvinia molesta*. *J. Environ. Chem. Eng.* **2019**, *7*, 102857. [[CrossRef](#)]
28. Taherdanak, M.; Zilouei, H.; Karimi, K. The influence of dilute sulfuric acid pretreatment on biogas production from wheat plant. *Int. J. Green Energy* **2016**, *13*, 1129–1134. [[CrossRef](#)]
29. Loow, Y.-L.; Wu, T.Y.; Jamaliah, M.J.; Mohammad, A.W.; Teoh, W.H. Typical conversion of lignocellulosic biomass into reducing sugars using dilute acid hydrolysis and alkaline pretreatment. *Cellulose* **2016**, *23*, 1491–1520. [[CrossRef](#)]
30. Watthier, E.; Andreani, C.L.; Torres, D.G.B.; Kuczman, O.; Tavares, M.H.F.; Lopes, D.D.; Gomes, S.D. Cassava Wastewater Treatment in Fixed-Bed Reactors: Organic Matter Removal and Biogas Production. *Front. Sustain. Food Syst.* **2019**, *3*, 6. [[CrossRef](#)]
31. Costa, R.C.; Ramos, M.D.N.; Fleck, L.; Gomes, S.D.; Aguiar, A. Critical analysis and predictive models using the physicochemical characteristics of cassava processing wastewater generated in Brazil. *J. Water Process Eng.* **2022**, *47*, 102629. [[CrossRef](#)]
32. Kong, X.; Niu, J.; Zhang, W.; Liu, J.; Yuan, J.; Li, H.; Yue, X. Mini art review for zero valent iron application in anaerobic digestion and technical bottlenecks. *Sci. Total Environ.* **2021**, *791*, 148415. [[CrossRef](#)]
33. Kannah, R.Y.; Kavitha, S.; Rajesh Banu, J.; Yeom, I.T.; Johnson, M. Synergetic effect of combined pretreatment for energy efficient biogas generation. *Bioresour. Technol.* **2017**, *232*, 235–246. [[CrossRef](#)]
34. Kouas, M.; Torrijos, M.; Sousbie, P.; Harmand, J.; Sayadi, S. Modeling the anaerobic co-digestion of solid waste: From batch to semi-continuous simulation. *Bioresour. Technol.* **2019**, *274*, 33–42. [[CrossRef](#)] [[PubMed](#)]
35. Elagroudy, S.; Radwan, A.G.; Banadda, N.; Mostafa, N.G.; Owusu, P.A.; Janajreh, I. Mathematical models comparison of biogas production from anaerobic digestion of microwave pretreated mixed sludge. *Renew. Energy* **2020**, *155*, 1009–1020. [[CrossRef](#)]
36. Zaidi, A.A.; Feng, R.; Malik, A.; Khan, S.Z.; Shi, Y.; Bhutta, A.J.; Shah, A.H. Combining Microwave Pretreatment with Iron Oxide Nanoparticles Enhanced Biogas and Hydrogen Yield from Green Algae. *Processes* **2019**, *7*, 24. [[CrossRef](#)]
37. Zaidi, A.A.; RuiZhe, F.; Malik, A.; Khan, S.Z.; Bhutta, A.J.; Shi, Y.; Mushtaq, K. Conjoint effect of microwave irradiation and metal nanoparticles on biogas augmentation from anaerobic digestion of green algae. *Int. J. Hydrog. Energy* **2019**, *44*, 14661–14670. [[CrossRef](#)]
38. Daiem, M.M.A.; Hatata, A.; Galal, O.H.; Said, N.; Ahmed, D. Prediction of biogas production from anaerobic co-digestion of waste activated sludge and wheat straw using two-dimensional mathematical models and an artificial neural network. *Renew. Energy* **2021**, *178*, 226–240. [[CrossRef](#)]
39. Salehi, R.; Yuan, Q.; Chaiprapat, S. Development of Data-Driven Models to Predict Biogas Production from Spent Mushroom Compost. *Agriculture* **2022**, *12*, 1090. [[CrossRef](#)]
40. American Public Health, A. APHA standard methods for the examination of water and wastewater. In *Standard Methods for the Examination of Water & Wastewater*; American Public Health Association: Washington, DC, USA, 2005.

41. Cremonez, P.A.; Sampaio, S.C.; Teleken, J.G.; Weiser Meier, T.; Dieter, J.; Teleken, J. Influence of inoculum to substrate ratio on the anaerobic digestion of a cassava starch polymer. *Ind. Crops Prod.* **2019**, *141*, 111709. [[CrossRef](#)]
42. Lavine, B.K.; Auslander, G.; Ritter, J. Polarographic studies of zero valent iron as a reductant for remediation of nitroaromatics in the environment. *Microchem. J.* **2001**, *70*, 69–83. [[CrossRef](#)]
43. Bang, S.; Johnson, M.D.; Korfiatis, G.P.; Meng, X. Chemical reactions between arsenic and zero-valent iron in water. *Water Res.* **2005**, *39*, 763–770. [[CrossRef](#)] [[PubMed](#)]
44. Zerrouki, S.; Rihani, R.; Lekikot, K.; Ramdhane, I. Enhanced biogas production from anaerobic digestion of wastewater from the fruit juice industry by sonolysis: Experiments and modelling. *Water Sci. Technol.* **2021**, *84*, 644–655. [[CrossRef](#)]
45. Das, A.; Mondal, C.; Roy, S. Kinetic Study of Biogas Recovery from Thermo-chemically Pre-treated Rice Husk. *Indian Chem. Eng.* **2018**, *60*, 297–313. [[CrossRef](#)]
46. Dong, D.; Kyung Choi, O.; Woo Lee, J. Influence of the continuous addition of zero valent iron (ZVI) and nano-scaled zero valent iron (nZVI) on the anaerobic biomethanation of carbon dioxide. *Chem. Eng. J.* **2022**, *430*, 132233. [[CrossRef](#)]
47. Xi, Y.; Mallavarapu, M.; Naidu, R. Reduction and adsorption of Pb²⁺ in aqueous solution by nano-zero-valent iron—A SEM, TEM and XPS study. *Mater. Res. Bull.* **2010**, *45*, 1361–1367. [[CrossRef](#)]
48. Boontian, N.; Phorndon, T.; Piasai, C.; Padri, M. Combination of Alkaline and Heat Pretreatments with Zero-Valent Iron Application in Cassava Pulp and Wastewater for Methane Generation: Development from Batch to Continuous Systems. *Fermentation* **2023**, *9*, 108. [[CrossRef](#)]
49. Boontian, N. Effect of Zero Valent Iron (ZVI) in Wastewater Treatment: A Review. *Appl. Mech. Mater.* **2015**, *775*, 180–184. [[CrossRef](#)]
50. Ullah, S.; Faiz, P.; Leng, S. Synthesis, Mechanism, and Performance Assessment of Zero-Valent Iron for Metal-Contaminated Water Remediation: A Review. *CLEAN–Soil Air Water* **2020**, *48*, 2000080. [[CrossRef](#)]
51. Li, J.; Tabassum, S. Effect of zero-valent iron and iron-carbon particles on the denitrification efficiency of anammox process under gradual cooling conditions. *Clean. Eng. Technol.* **2022**, *8*, 100477. [[CrossRef](#)]
52. Taherzadeh, M.J.; Karimi, K. Pretreatment of Lignocellulosic Wastes to Improve Ethanol and Biogas Production: A Review. *Int. J. Mol. Sci.* **2008**, *9*, 1621–1651. [[CrossRef](#)] [[PubMed](#)]
53. Virunanon, C.; Ouephanit, C.; Burapatana, V.; Chulalaksananukul, W. Cassava pulp enzymatic hydrolysis process as a preliminary step in bio-alcohols production from waste starchy resources. *J. Clean. Prod.* **2013**, *39*, 273–279. [[CrossRef](#)]
54. Mozhiarasi, V. Overview of pretreatment technologies on vegetable, fruit and flower market wastes disintegration and bioenergy potential: Indian scenario. *Chemosphere* **2022**, *288*, 132604. [[CrossRef](#)] [[PubMed](#)]
55. Zhen, G.; Lu, X.; Kato, H.; Zhao, Y.; Li, Y.-Y. Overview of pretreatment strategies for enhancing sewage sludge disintegration and subsequent anaerobic digestion: Current advances, full-scale application and future perspectives. *Renew. Sustain. Energy Rev.* **2017**, *69*, 559–577. [[CrossRef](#)]
56. Carrere, H.; Antonopoulou, G.; Affes, R.; Passos, F.; Battimelli, A.; Lyberatos, G.; Ferrer, I. Review of feedstock pretreatment strategies for improved anaerobic digestion: From lab-scale research to full-scale application. *Bioresour. Technol.* **2016**, *199*, 386–397. [[CrossRef](#)]
57. Puyol, D.; Flores-Alsina, X.; Segura, Y.; Molina, R.; Padrino, B.; Fierro, J.L.G.; Gernaey, K.V.; Melero, J.A.; Martinez, F. Exploring the effects of ZVI addition on resource recovery in the anaerobic digestion process. *Chem. Eng. J.* **2018**, *335*, 703–711. [[CrossRef](#)]
58. Zhao, Z.; Zhang, Y.; Li, Y.; Quan, X.; Zhao, Z. Comparing the mechanisms of ZVI and Fe₃O₄ for promoting waste-activated sludge digestion. *Water Res.* **2018**, *144*, 126–133. [[CrossRef](#)]
59. Fox, M.H.; Noike, T.; Ohki, T. Alkaline subcritical-water treatment and alkaline heat treatment for the increase in biodegradability of newsprint waste. *Water Sci. Technol.* **2003**, *48*, 77–84. [[CrossRef](#)]
60. Şenol, H.; Açıkel, Ü.; Demir, S.; Oda, V. Anaerobic digestion of cattle manure, corn silage and sugar beet pulp mixtures after thermal pretreatment and kinetic modeling study. *Fuel* **2020**, *263*, 116651. [[CrossRef](#)]
61. Kor-Bicakci, G.; Ubay-Cokgor, E.; Eskicioglu, C. Effect of dewatered sludge microwave pretreatment temperature and duration on net energy generation and biosolids quality from anaerobic digestion. *Energy* **2019**, *168*, 782–795. [[CrossRef](#)]
62. Sumardiono, S.; Budiyo; Mardiani, D.T. The effect of microwave power and heating time pretreatment on biogas production from fresh and dried water hyacinth (*Eichhornia crassipes*). *AIP Conf. Proc.* **2015**, *1699*, 050018. [[CrossRef](#)]
63. Mirmasoumi, S.; Khoshbakhti Saray, R.; Ebrahimi, S. Evaluation of thermal pretreatment and digestion temperature rise in a biogas fueled combined cooling, heat, and power system using exergo-economic analysis. *Energy Convers. Manag.* **2018**, *163*, 219–238. [[CrossRef](#)]
64. McVoitte, W.P.A.; Clark, O.G. The effects of temperature and duration of thermal pretreatment on the solid-state anaerobic digestion of dairy cow manure. *Heliyon* **2019**, *5*, e02140. [[CrossRef](#)] [[PubMed](#)]
65. Shangdiar, S.; Lin, Y.-C.; Ponnusamy, V.K.; Wu, T.-Y. Pretreatment of lignocellulosic biomass from sugar bagasse under microwave assisted dilute acid hydrolysis for biobutanol production. *Bioresour. Technol.* **2022**, *361*, 127724. [[CrossRef](#)]
66. Aruwajoye, G.S.; Faloye, F.D.; Kana, E.G. Soaking assisted thermal pretreatment of cassava peels wastes for fermentable sugar production: Process modelling and optimization. *Energy Convers. Manag.* **2017**, *150*, 558–566. [[CrossRef](#)]
67. Antonopoulou, G.; Lyberatos, G. Effect of Pretreatment of Sweet Sorghum Biomass on Methane Generation. *Waste Biomass Valorization* **2013**, *4*, 583–591. [[CrossRef](#)]

68. Liu, T.; Wu, C.; Wang, Y.; Xue, G.; Zhang, M.; Liu, C.; Zheng, Y. Enhanced Deep Utilization of Low-Organic Content Sludge by Processing Time-Extended Low-Temperature Thermal Pretreatment. *ACS Omega* **2021**, *6*, 28946–28954. [[CrossRef](#)]
69. Liu, X.; Xu, Q.; Wang, D.; Yang, Q.; Wu, Y.; Li, Y.; Fu, Q.; Yang, F.; Liu, Y.; Ni, B.-J.; et al. Thermal-alkaline pretreatment of polyacrylamide flocculated waste activated sludge: Process optimization and effects on anaerobic digestion and polyacrylamide degradation. *Bioresour. Technol.* **2019**, *281*, 158–167. [[CrossRef](#)]
70. Wyman, C.E.; Dale, B.E.; Elander, R.T.; Holtzapple, M.; Ladisch, M.R.; Lee, Y.Y. Coordinated development of leading biomass pretreatment technologies. *Bioresour. Technol.* **2005**, *96*, 1959–1966. [[CrossRef](#)]
71. Feng, Y.; Zhang, Y.; Quan, X.; Chen, S. Enhanced anaerobic digestion of waste activated sludge digestion by the addition of zero valent iron. *Water Res.* **2014**, *52*, 242–250. [[CrossRef](#)]
72. Liu, Y.; Zhang, Y.; Quan, X.; Li, Y.; Zhao, Z.; Meng, X.; Chen, S. Optimization of anaerobic acidogenesis by adding Fe⁰ powder to enhance anaerobic wastewater treatment. *Chem. Eng. J.* **2012**, *192*, 179–185. [[CrossRef](#)]
73. Zhang, J.; Qu, Y.; Qi, Q.; Zhang, P.; Zhang, Y.; Tong, Y.W.; He, Y. The bio-chemical cycle of iron and the function induced by ZVI addition in anaerobic digestion: A review. *Water Res.* **2020**, *186*, 116405. [[CrossRef](#)] [[PubMed](#)]
74. Deng, S.; Li, D.; Yang, X.; Xing, W.; Li, J.; Zhang, Q. Biological denitrification process based on the Fe(0)–carbon micro-electrolysis for simultaneous ammonia and nitrate removal from low organic carbon water under a microaerobic condition. *Bioresour. Technol.* **2016**, *219*, 677–686. [[CrossRef](#)] [[PubMed](#)]
75. Honetschlägerová, L.; Škarohlíd, R.; Martinec, M.; Šír, M.; Luciano, V. Interactions of nanoscale zero valent iron and iron reducing bacteria in remediation of trichloroethene. *Int. Biodeterior. Biodegrad.* **2018**, *127*, 241–246. [[CrossRef](#)]
76. Kumar, N.; Auffan, M.; Gattacceca, J.; Rose, J.; Olivi, L.; Borschneck, D.; Kvapil, P.; Jublot, M.; Kaifas, D.; Malleret, L.; et al. Molecular Insights of Oxidation Process of Iron Nanoparticles: Spectroscopic, Magnetic, and Microscopic Evidence. *Environ. Sci. Technol.* **2014**, *48*, 13888–13894. [[CrossRef](#)]
77. Ren, X.; Chen, Y.; Guo, L.; She, Z.; Gao, M.; Zhao, Y.; Shao, M. The influence of Fe²⁺, Fe³⁺ and magnet powder (Fe₃O₄) on aerobic granulation and their mechanisms. *Ecotoxicol. Environ. Saf.* **2018**, *164*, 1–11. [[CrossRef](#)]
78. Zhu, Y.; Zhao, Z.; Yang, Y.; Zhang, Y. Dual roles of zero-valent iron in dry anaerobic digestion: Enhancing interspecies hydrogen transfer and direct interspecies electron transfer. *Waste Manag.* **2020**, *118*, 481–490. [[CrossRef](#)]
79. Wang, C.; Wei, W.; Dai, X.; Ni, B.-J. Zero valent iron greatly improves sludge destruction and nitrogen removal in aerobic sludge digestion. *Chem. Eng. J.* **2022**, *433*, 134459. [[CrossRef](#)]
80. Li, L.; Kong, X.; Yang, F.; Li, D.; Yuan, Z.; Sun, Y. Biogas Production Potential and Kinetics of Microwave and Conventional Thermal Pretreatment of Grass. *Appl. Biochem. Biotechnol.* **2012**, *166*, 1183–1191. [[CrossRef](#)]
81. Pavlostathis, S.G.; Giraldo-Gomez, E. Kinetics of anaerobic treatment: A critical review. *Crit. Rev. Environ. Control* **1991**, *21*, 411–490. [[CrossRef](#)]
82. Donoso-Bravo, A.; Pérez-Elvira, S.I.; Fdz-Polanco, F. Application of simplified models for anaerobic biodegradability tests. Evaluation of pre-treatment processes. *Chem. Eng. J.* **2010**, *160*, 607–614. [[CrossRef](#)]
83. Rajput, A.A.; Zeshan; Visvanathan, C. Effect of thermal pretreatment on chemical composition, physical structure and biogas production kinetics of wheat straw. *J. Environ. Manag.* **2018**, *221*, 45–52. [[CrossRef](#)] [[PubMed](#)]
84. Abdelwahab, T.A.M.; Mohanty, M.K.; Sahoo, P.K.; Behera, D. Metal nanoparticle mixtures to improve the biogas yield of cattle manure. *Biomass Convers. Biorefinery* **2023**, *13*, 2243–2254. [[CrossRef](#)]
85. Deepanraj, B.; Sivasubramanian, V.; Jayaraj, S. Kinetic study on the effect of temperature on biogas production using a lab scale batch reactor. *Ecotoxicol. Environ. Saf.* **2015**, *121*, 100–104. [[CrossRef](#)] [[PubMed](#)]
86. Pardilhó, S.; Pires, J.C.; Boaventura, R.; Almeida, M.; Maia Dias, J. Biogas production from residual marine macroalgae biomass: Kinetic modelling approach. *Bioresour. Technol.* **2022**, *359*, 127473. [[CrossRef](#)]
87. Ap, Y.; Farghali, M.; Mohamed, I.M.A.; Iwasaki, M.; Tangtaweewipat, S.; Ihara, I.; Sakai, R.; Umetsu, K. Potential of biogas production from the anaerobic digestion of *Sargassum fulvellum* macroalgae: Influences of mechanical, chemical, and biological pretreatments. *Biochem. Eng. J.* **2021**, *175*, 108140. [[CrossRef](#)]
88. Nielfa, A.; Cano, R.; Fdz-Polanco, M. Theoretical methane production generated by the co-digestion of organic fraction municipal solid waste and biological sludge. *Biotechnol. Rep.* **2015**, *5*, 14–21. [[CrossRef](#)]
89. Patowary, D.; Baruah, D.C. Effect of combined chemical and thermal pretreatments on biogas production from lignocellulosic biomasses. *Ind. Crops Prod.* **2018**, *124*, 735–746. [[CrossRef](#)]
90. David, R.J.; Helbling Damian, E.; Lee Tae, K.; Park, J.; Fenner, K.; Kohler Hans-Peter, E.; Ackermann, M. Association of Biodiversity with the Rates of Micropollutant Biotransformations among Full-Scale Wastewater Treatment Plant Communities. *Appl. Environ. Microbiol.* **2015**, *81*, 666–675. [[CrossRef](#)]
91. Wu, P.; Li, L.; Jiang, J.; Sun, Y.; Yuan, Z.; Feng, X.; Guo, Y. Effects of fermentative and non-fermentative additives on silage quality and anaerobic digestion performance of *Pennisetum purpureum*. *Bioresour. Technol.* **2020**, *297*, 122425. [[CrossRef](#)]

Disclaimer/Publisher’s Note: The statements, opinions and data contained in all publications are solely those of the individual author(s) and contributor(s) and not of MDPI and/or the editor(s). MDPI and/or the editor(s) disclaim responsibility for any injury to people or property resulting from any ideas, methods, instructions or products referred to in the content.